Afyon Kocatepe Üniversitesi Fen ve Mühendislik Bilimleri Dergisi
Afyon Kocatepe University – Journal of Science and Engineering
https://dergipark.org.tr/tr/pub/akufemubid

Araştırma Makalesi / Research Article
e-ISSN: 2149-3367
DOI: https://doi.org/10.35414/akufemubid.1537900
AKÜ FEMÜBİD **25** (2025) 061102 (1279-1290)
AKU J. Sci. Eng. **25** (2025) 061102 (1279-1290)

Investigation of Optimized Density of States (DOS) Analysis, UV-Visible Spectroscopy, NMR Spectroscopy, and Molecular Electrostatic Potential (MEP) Mapping of Ru-486 and Its Derivatives

***Makale Bilgisi / Article Info**
Alındı/Received: 23.08.2024
Kabul/Accepted: 28.06.2025
Yayımlandı/Published: xx.xx.xxxx

Ru-486 ve Türevlerinin Optimize Edilmiş Durum Yoğunluğu (DOS) Analizi, UV-Görünür Bölge Spektroskopisi, NMR Spektroskopisi ve Moleküler Elektrostatik Potansiyel (MEP) Haritalaması Üzerine İnceleme

Mehmet Hanifi KEBİROĞLU[1,2*], Fermin AK[1]

[1]Malatya Turgut Özal University, Darende Bekir Ilıcak Vocational School, Dept.of Medical Services and Techniques/Opticianry Pr., Malatya, Türkiye
[2]Fırat University, Faculty of Science, Department of Physics, 23119, Elazığ, Türkiye

Abstract
When used in combination with misoprostol, RU-486 (Mifepristone) offers a highly effective and non-invasive option for managing early pregnancy loss (EPL), providing a suitable alternative to surgical interventions. In this study, quantum computational chemistry methods were employed to calculate the structural and spectroscopic properties of the Ru-486 molecule and its derivatives (CH_2CH_3, CH_3, F). The molecule was optimized using Density Functional Theory (DFT/B3LYP) with the B3LYP/6-31G basis set. Density of States (DOS) Analysis, UV-Visible Spectroscopy, NMR Spectroscopy, and Molecular Electrostatic Potential (MEP) Mapping were investigated. The compound exhibited HOMO-LUMO band gaps ranging from 3.19 to 4.02 eV, with principal vibrational peaks at 3076 cm^{-1} observed in the FT-IR spectrum and maximum UV absorption detected at 408 nm. Additionally, a discussion of the basic theory behind the characterization methods is included.

***Keywords:** Ru-486, DOS, UV-Vis, NMR, MEP*

Öz
Misoprostol ile birlikte kullanıldığında, Ru-486 (Mifepriston) erken gebelik kaybının (EGK) yönetiminde son derece etkili ve invaziv olmayan bir seçenek sunarak cerrahi müdahalelere uygun bir alternatif sağlar. Bu çalışmada, Ru-486 molekülü ve türevlerinin (CH_2CH_3, CH3, F) yapısal ve spektroskopik özelliklerini hesaplamak için kuantum hesaplamalı kimya yöntemleri kullanılmıştır. Molekül, B3LYP/6-31G baz seti ile Yoğunluk Fonksiyonel Teorisi (DFT/B3LYP) kullanılarak optimize edilmiştir. Durum Yoğunluğu (DOS) Analizi, UV-Görünür Bölge Spektroskopisi, NMR Spektroskopisi ve Moleküler Elektrostatik Potansiyel (MEP) Haritalaması incelenmiştir. HOMO-LUMO bant aralıkları 3,19–4,02 eV arasında belirlenen bileşiğin FT-IR spektrumunda temel titreşim pikleri 3076 cm^{-1} değerinde gözlenmiş olup, UV-Vis analizinde maksimum absorpsiyon 408 nm dalga boyunda tespit edilmiştir. Ayrıca, karakterizasyon yöntemlerinin temel teorisi üzerine bir tartışma da dahil edilmiştir.

***Anahtar Kelimeler:** Ru-486, DOS, UV-Vis, NMR, MEP*

1. Introduction

Early pregnancy loss (EPL), commonly known as miscarriage, refers to spontaneously losing a pregnancy before 20 weeks of gestation (Yang et al., 2024). It is a frequent complication of pregnancy, affecting about 10-15% of clinically recognized pregnancies (McCullya et al., 20242024). Most EPL cases occur during the first trimester, before the 12th week of pregnancy (Riddell 2024). EPL can be emotionally and physically challenging for women and their families, and understanding its management is critical for healthcare providers (George-Carey et al., 2024). EPL can result from various factors, including genetic abnormalities, hormonal imbalances, uterine anomalies, infections, and lifestyle factors (Tisato et al., 2024).

Chromosomal abnormalities, such as trisomy or monosomy, are the most common cause, accounting for approximately half of all early miscarriages (Qin et al., 2024). Other contributing factors may include advanced maternal age, a history of previous miscarriages, and underlying medical conditions such as polycystic ovary syndrome (PCOS) or thyroid disorders (La Marca & Diamanti, 2024). Ru-486, also known as Mifepristone, is a medication widely used in the medical management of early pregnancy loss (Turner et al., 2024). Ru-486 functions as an antiprogestogen by binding to

**Sorumlu Yazar/Corresponding Author: Mehmet Hanifi KEBİROĞLU* *e-posta/e-mail: hanifi.kebiroglu@ozal.edu.tr*

progesterone receptors and inhibiting the action of progesterone, a hormone crucial for maintaining pregnancy (Elia et al., 2024). Without sufficient progesterone, the uterine lining breaks down, leading to the termination of the pregnancy. Ru-486 is often used in combination with a prostaglandin analog, such as misoprostol, to enhance uterine contractions and facilitate the expulsion of pregnancy tissue (Marwah et al., 2016). This combination is highly effective and offers a non-surgical option for managing EPL, providing women with a choice in their care (Chua et al., 2024). Progesterone Receptor Antagonism: Ru-486 competes with progesterone for binding to its receptors in the uterus and placenta, leading to the detachment of the trophoblast and decidua (Ye et al., 2024). Cervical Ripening: Ru-486 induces cervical softening and dilation, which helps in the expulsion process.

Enhancement of Uterine Contractions: When used with misoprostol, Ru-486 increases the frequency and intensity of uterine contractions, aiding in the complete evacuation of the uterus (Hogmark 2024). Ru-486 is administered under medical supervision, typically in a clinic or hospital setting. The standard regimen involves an initial dose of Ru-486 followed by misoprostol 24-48 hours later. Clinical studies have shown this regimen is highly effective, with success rates of over 95% in inducing complete abortion in early pregnancy (Biswas et al., 2024). Non-Invasive: It provides a non-surgical alternative to procedures like dilation and curettage (D&C) (Viganò et al., 2024). Privacy and Comfort: Women can undergo the process in a more private and comfortable setting, often at home (Bae & Kim, 2024). High Efficacy: The combination of Ru-486 and misoprostol has a high success rate for complete uterine evacuation (Akter et al., 2024). The emotional impact of EPL can be significant, and the use of Ru-486 does not mitigate the need for psychological support (Statham 2002). Counseling and support groups are essential components of care to help women and their families cope with the loss and the medical process (Pedraza et al., 2024). Ongoing research aims to optimize the use of Ru-486 and explore its potential applications in various reproductive health contexts (Elia et al., 2024). Studies are focusing on refining dosing regimens, minimizing side effects, and understanding the long-term outcomes of medical management with Ru-486 (Kay et al., 2024). Additionally, research into patient experiences and preferences continues to inform best practices for managing EPL with medical methods (Engstrom et al., 2024).

This study demonstrates how small analytical modifications (CH_2CH_3, CH_3, F) that can fine-tune the electron-distribution of RU-486 aim to systematically reveal the fundamental electronic distribution (HOMO-LUMO gap, dipole moment, reactivity indices) that may underlie pharmacological performance.

2. Materials and Methods

Ab initio methods and Density Functional Theory (DFT) are the cornerstones of quantum chemistry used to solve the electronic Schrödinger equation that governs the behavior of electrons in atoms and molecules (Rahman et al., 2024). Accurate determination of molecular properties such as geometry, energy, and electronic distribution depends on these methods. Ab Initio Methods: Ab initio methods derived from first principles are not based on experimental data (Lewars 2024). These include post-Hartree-Fock methods such as Hartree-Fock (HF) and Møller-Plesset distortion theory (MP2), Coupled Cluster (CC), and Configuration Interaction (CI). The main difficulty with ab initio methods is the computational cost, which increases rapidly with system size. Density Functional Theory (DFT): Unlike ab initio methods, DFT is based on the electron density rather than the wave function (Genoni & Martín Pendás, 2024).

The Hohenberg-Kohn theorems establish that the ground state properties of a system are uniquely determined by the electron density. DFT is computationally less expensive than ab initio methods, making it widely used for larger systems (Pellegrini & Sanna, 2024). However, the accuracy of DFT calculations depends heavily on the choice of exchange-correlation functional. 6-31G includes additional functions to better represent valence electrons, such as Split-Valence Basis Sets (Butera 2024). Comprehensive quantum chemical computations were carried out using the B3LYP-DFT methodology with the 6-31G(d) basis set, as implemented in the Gaussian 05 software package (Gidado et al., 2024). This method was also employed to calculate the ^{1}H and ^{13}C chemical shifts for the Ru-486 molecule and its derivatives (CH_2CH_3, CH_3, F) utilizing the Gauge-Independent Atomic Orbital (GIAO) approach (Nguyen et al., 2024). Additionally, basic vibrational frequencies were determined, and the geometrical parameters were optimized at the same theoretical level (Tegegn et al., 2024).

3. Results and Discussions

3.1. *Geometry Optimization*

Geometry optimization is a two-step process to determine the three-dimensional spatial arrangement of atoms in a molecule (Margraf 2024). In this process, the first step is to determine the initial geometry of the molecule and the second step is to optimize this geometry by energy minimization. These processes are performed to find the lowest energy conformation of the molecule and are usually performed using quantum chemistry software. Gaussian 09 software is a powerful tool widely used to perform such geometry optimizations (Tegegn et al., 2024). Using Gaussian 09 software, geometry optimization was performed on the pure Ru-486 molecule. In addition, optimized geometry states were determined by adding various components to the Ru-486 molecule (CH_2CH_3, CH_3, F). These additional components allow different conformations to be obtained by changing the structural properties and energy states of the molecule. At each step in the molecular optimization process, an energy change occurs (Yılmaz & Kebiroglu, 2024). The optimized structures of the investigated compounds were obtained because of molecular-level interactions and energy minimizations (Reeda et al., 2024). These structures represent the most stable and lowest energy states of the molecules. These structures obtained because of optimization processes play an important role in understanding molecular properties and examining the mechanisms of chemical reactions. Optimization results are shown in Figure 1 and Table 1.

Table 1. Summary of Optimized Geometric Structures and Electronic Properties of Undoped and Doped Ru-486 Molecules

Molecule	Description
Undoped Ru-486	Represents the optimized geometry of the pure, undoped Ru-486 molecule. The molecular structure consists of carbon (C), hydrogen (H), oxygen (O), and nitrogen (N) atoms in 3D configuration. Oxygen atoms are red, and nitrogen atoms are blue.
CH_2CH_3 Doped Ru-486	Shows the Ru-486 molecule doped with an ethyl group (CH_2CH_3). The ethyl group changes the overall geometry and electronic properties. The optimized structure illustrates the integration of the ethyl group into the Ru-486 framework, affecting the spatial arrangement of atoms.
CH_3 Doped Ru-486	Displays the Ru-486 molecule doped with a methyl group (CH_3). The addition of the methyl group alters the molecular structure. The optimized geometry shows the position of the methyl group and its impact on the molecule's overall conformation.
F Doped Ru-486	Depicts the Ru-486 molecule doped with a fluorine atom (F). Incorporating the fluorine atom significantly influences the electronic distribution and geometry. The optimized structure shows the placement of the fluorine atom (light green) within the molecular framework.

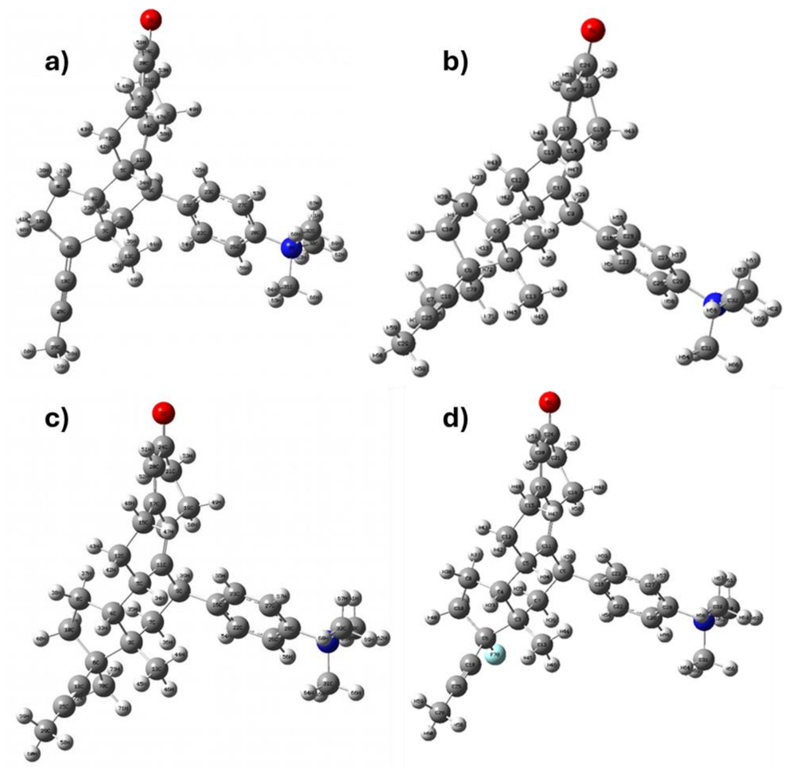

Figure 1. Optimized structure of Ru-486 molecule a) undoped b) CH_2CH_3 c) CH_3 d) F doped.

3.2. *Molecular Electrostatic Potential (MEP) Maps*

Electrostatic potential maps (MEP) are a vital tool for analyzing the distribution of electronegativity and partial charges on different atoms within a molecule (Suhta et al., 2024). In MEP (Molecular Electrostatic Potential), the red regions indicate areas of negative charge, suggesting susceptibility to electrophilic attack, while the blue regions indicate areas of positive charge, indicating a propensity for nucleophilic attack, as shown (Çankaya et al., 2024). This analysis is essential for understanding various properties of a molecule, including its bonding interactions with biological molecules (Holehouse &

Kragelund, 2024). These interactions can involve charge-dipole, dipole-dipole, and quadrupole-dipole interactions. The MEP map visually represents electron acceptor, donor, and neutral regions of a molecule, which helps in identifying the electrophilic and nucleophilic reactive regions. The surface map is typically color-coded, ranging from red to blue, indicating regions from electron-rich (red) to electron-poor (blue). In the MEP analysis, the green color represents areas where the electron density is moderate. Molecular electrostatic potential illustrates electronic density and is valuable for identifying sites susceptible to electrophilic and nucleophilic attacks and for understanding hydrogen bonding interactions (Kebiroglu & Ak, 2023). For the Ru-486 molecule, some observed that the regions around the remaining part of the molecule are less electron-dense, indicated by green. The green-colored areas show that the C-H hydrogens are in the electrophilic region. This color-coding allows for a clear identification of the electrophilic and nucleophilic regions, which is crucial for predicting the molecule's interactions with other molecules during chemical reactions. The analysis indicated that the Ru-486 molecule and its derivatives usually exhibit more nucleophilic properties compared to electrophilic properties. The MEP maps for the Ru-486 molecule and its derivatives is displayed in Figure 2 and in Table 2. These maps illustrate the electron density distribution, helping to visualize the potential reactive sites of the molecules and providing insights into their chemical behavior.

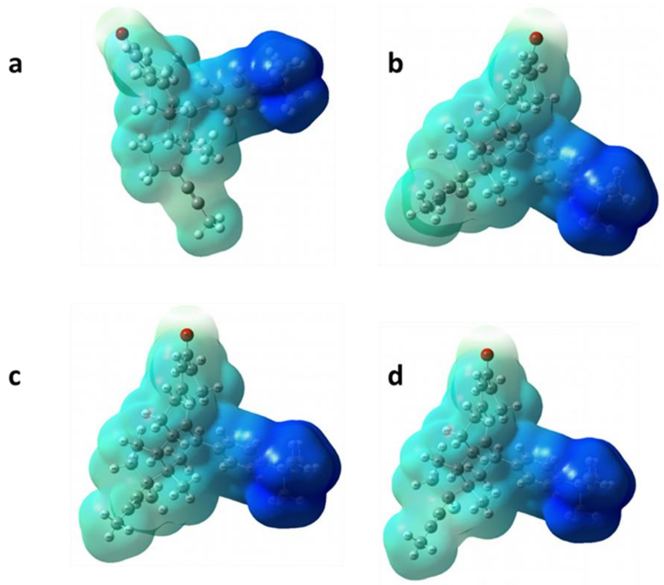

Figure 2. MEP maps of a) Ru-486, b) Ru-486-CH_2CH_3, c) Ru-486-CH_3, d) Ru-486-F molecules

Table 2. Summary of Molecular Electrostatic Potential (MEP) Maps for Ru-486 and its derivatives

Molecule	Description	Electron-Rich Regions (Red)	Electron-Poor Regions (Blue)	Effect of Doping
Ru-486	Electrostatic potential surface of the pure Ru-486 molecule.	Around electronegative atoms like oxygen, indicating high electrophilic attack likelihood.	Regions indicating nucleophilic sites.	Baseline for comparison, showing natural electron distribution without any modifications.
Ru-486-CH_2CH_3 (Ethyl)	MEP map of Ru-486 molecule doped with an ethyl group (CH_2CH_3).	Shifted due to the influence of the ethyl group.	Shifted areas of nucleophilic sites compared to the undoped molecule.	The ethyl group alters the distribution, affecting the molecule's reactive regions.
Ru-486-CH_3 (Methyl)	MEP map of Ru-486 molecule doped with a methyl group (CH_3).	Similar shifts to those seen with the ethyl group but with less intensity.	Modifications in nucleophilic regions, less pronounced than with ethyl.	The methyl group also alters the electron distribution but to a lesser extent than the ethyl group.
Ru-486-F (Fluorine)	MEP map of Ru-486 molecule doped with a fluorine atom (F).	Strong red regions around fluorine, indicating significant electron density.	Distinct blue regions elsewhere, more prone to nucleophilic attack.	Fluorine significantly impacts the molecule, creating a unique electrostatic potential surface.

3.3. *Vibrational Spectroscopic Analysis Spectrum*

If the dipole moment of a molecule changes during vibration, the usual vibrational mode becomes infrared-active (i.e., absorbs incoming infrared light) (Alejandro et al., 2024). Therefore, symmetric vibrations are rarely observed in the infrared spectrum. If a molecule has a center of symmetry, all vibrations symmetric to this center are inactive in the infrared spectrum (Kolek et al., 2024). But asymmetric vibrations can be detected for all molecules. This lack of selectivity allows us to investigate the properties of most chemical groups in a single sample, especially amino acids and water molecules, which are difficult to detect using conventional spectroscopic techniques. In this study, the vibrational spectra of Ru-486 and its derivatives were analyzed using the DFT/B3LYP method and the 6-31G basis set. Estimated IR spectra showing the absorption peaks of the examined molecules in the range of 3500-0 cm^{-1} were obtained. The frequencies in the figures are harmonic frequencies and are calculated by multiplying the harmonic frequencies for each calculation level by the appropriate scaling factor. The similarity of complexes indicates similarity in both spectrum and vibrational frequencies. According to the basic principles of vibrational spectroscopy, the vibrational frequency of a bond increases as the bond strength increases and the mass of the bond atom decreases. Table 3 provides a summary of the peak intensities and frequencies observed in the FT-IR spectra (Figure 3a to Figure 3d) for the Ru-486 molecule and its derivatives, highlighting the highest intensity peaks and associated low-level transmittance changes.

Table 3. Summary of Peak Intensities and Frequencies in Figure 3a to Figure 3d with Associated Low-Level Transmittance Changes

Figure	Peak Number with Highest Intensity	Wavenumber (cm^{-1})	Other Transmittance Numbers with Low-Level Changes
Figure 3a	5	3076	84, 25, 35, 16, 22, 51, 53, 68, 85, 86
Figure 3b	1	3092	95, 36, 15, 22, 48, 54, 69, 84, 82, 90
Figure 3c	3	3092	94, 25, 36, 16, 22, 51, 67, 83, 84, 89
Figure 3d	8	3108	67, 26, 36, 15, 14, 27, 54, 64, 80, 82, 88

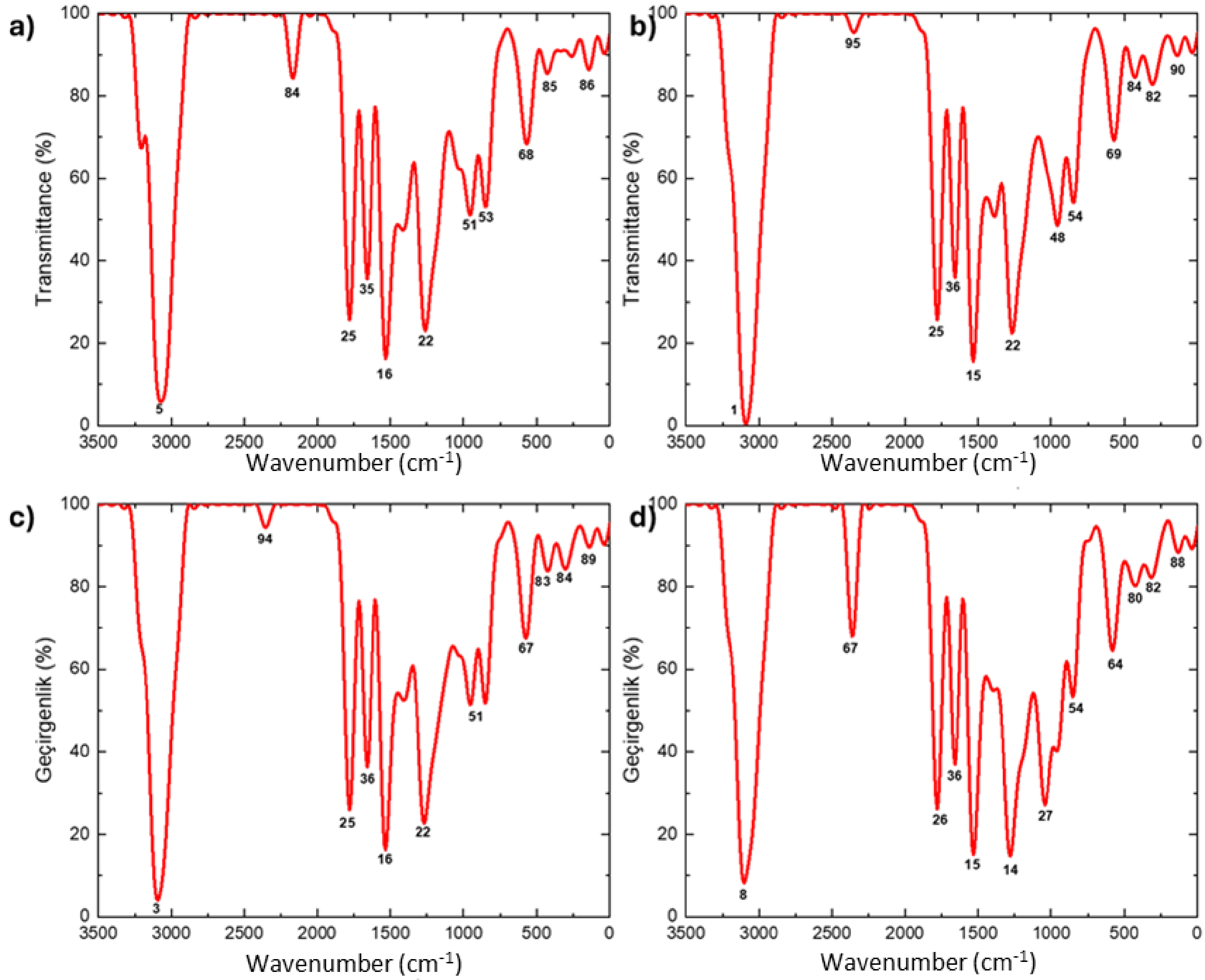

Figure 3. FT-IR spectrum of a) Ru-486, b) Ru-486-CH_2CH_3, c) Ru-486-CH_3, d) Ru-486-F molecules

3.4. *Nuclear Magnetic Resonance Spectroscopy*

3.4.1. *^{13}C NMR spectrum*

The ^{13}C NMR (Nuclear Magnetic Resonance) spectrum is a type of nuclear magnetic resonance spectroscopy used to determine the structure of organic compounds by identifying the different carbon environments in a molecule (Chakrawal et al., 2024). In the ^{13}C NMR spectrum of Ru-486 in Figure 4, mifepristone has a complex structure with various Ru-486 and its derivatives is given in Table 4.

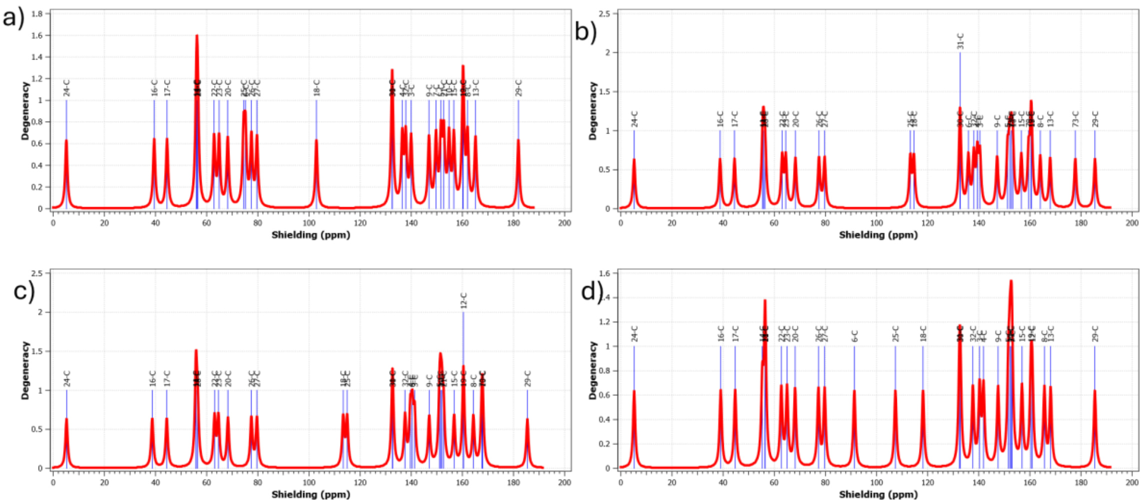

Figure 4. ^{13}C NMR spectrum of a) Ru-486, b) Ru-486-CH_2CH_3, c) Ru-486-CH_3, d) Ru-486-F molecules

Table 4. ^{13}C NMR spectra for Ru-486 and its derivatives

Compound	Region (ppm)	Peak Assignment
	0-50	Alkyl carbons (methylene CH_2 and methyl CH_3 groups)
Ru-486	50-100	Carbons attached to electronegative atoms, sp carbons, carbons connected to oxygen
(Mifepristone)	100-150	Aromatic and alkene carbons
	150-220	Carbonyl carbons (C=O)
	0-50	Ethyl group (CH_2 and CH_3) and other alkyl carbons
Ru-486-CH_2CH_3	50-100	Carbons attached to oxygen or nitrogen atoms
	100-150	Aromatic carbons
	150-220	Carbonyl carbons (C=O)
	0-50	Methyl group (CH_3) and other alkyl carbons
Ru-486-CH_3	50-100	Carbons attached to oxygen or nitrogen atoms
	100-150	Aromatic carbons
	150-220	Carbonyl carbons (C=O)
	0-50	Alkyl carbons
Ru-486-F	50-100	Carbons attached to fluorine atoms (de-shielding, downfield shift)
	100-150	Aromatic carbons
	150-220	Carbonyl carbons (C=O)

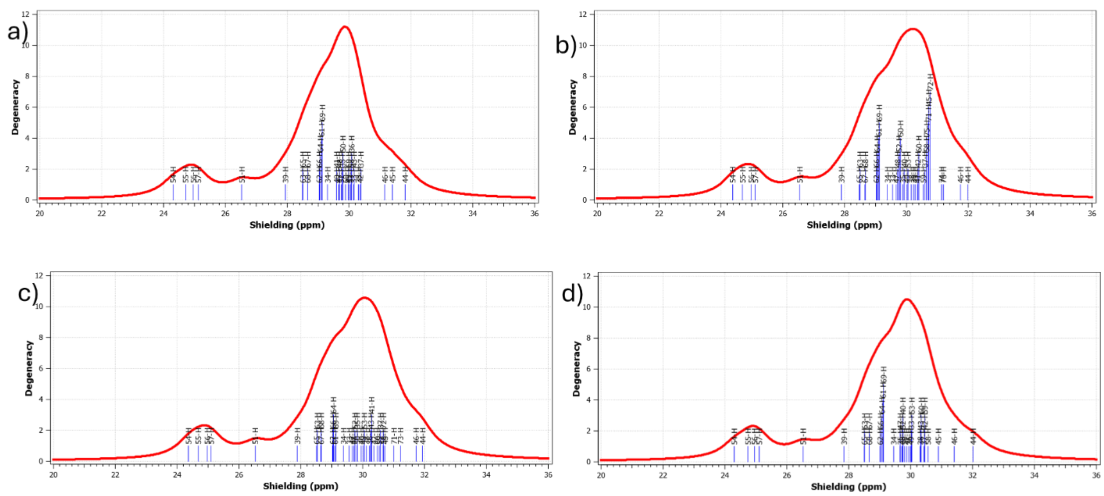

Figure 5. ^{1}H NMR spectrum of a) Ru-486, b) Ru-486-CH_2CH_3, c) Ru-486-CH_3, d) Ru-486-F molecules

3.4.2. *^{1}H NMR spectrum*

The ^{1}H NMR (Nuclear Magnetic Resonance) spectrum is a powerful technique used to determine the structure of organic compounds by identifying the different proton environments in a molecule (Tagliavini et al., 2024). In the 1H NMR spectrum of Ru-486 in Figure 5 and in Table 5.

Table 5. ^1H NMR spectra for Ru-486 and its derivatives

Compound	Region (ppm)	Peak Assignment
Ru-486	0-3	Alkyl protons (CH_2 and CH_3 groups), small peak around 1.0-2.5 ppm likely for methyl groups
	3-5	Protons attached to sp3 carbons adjacent to electronegative atoms (O, N)
	5-7	Olefinic protons (sp2 carbons in alkenes)
	6-9	Aromatic protons
	9-12	No significant peaks (absence of aldehyde or carboxylic acid protons)
Ru-486-CH_2CH_3	0-3	Alkyl protons, including ethyl group (CH_2 and CH_3), peaks around 1.0-2.5 ppm
	3-5	Protons attached to sp3 carbons adjacent to electronegative atoms (O, N)
	5-7	Olefinic protons (sp2 carbons in alkenes)
	6-9	Aromatic protons
	9-12	No significant peaks (absence of aldehyde or carboxylic acid protons)
Ru-486-CH_3	0-3	Alkyl protons, including methyl group (CH_3), peaks around 1.0-2.5 ppm
	3-5	Protons attached to sp3 carbons adjacent to electronegative atoms (O, N)
	5-7	Olefinic protons (sp2 carbons in alkenes)
	6-9	Aromatic protons
	9-12	No significant peaks (absence of aldehyde or carboxylic acid protons)
Ru-486-F	0-3	Alkyl protons (CH_2 and CH_3 groups), peaks around 1.0-2.5 ppm
	3-5	Protons attached to sp3 carbons adjacent to electronegative atoms (F)
	5-7	Olefinic protons (sp2 carbons in alkenes)
	6-9	Aromatic protons
	9-12	No significant peaks (absence of aldehyde or carboxylic acid protons)

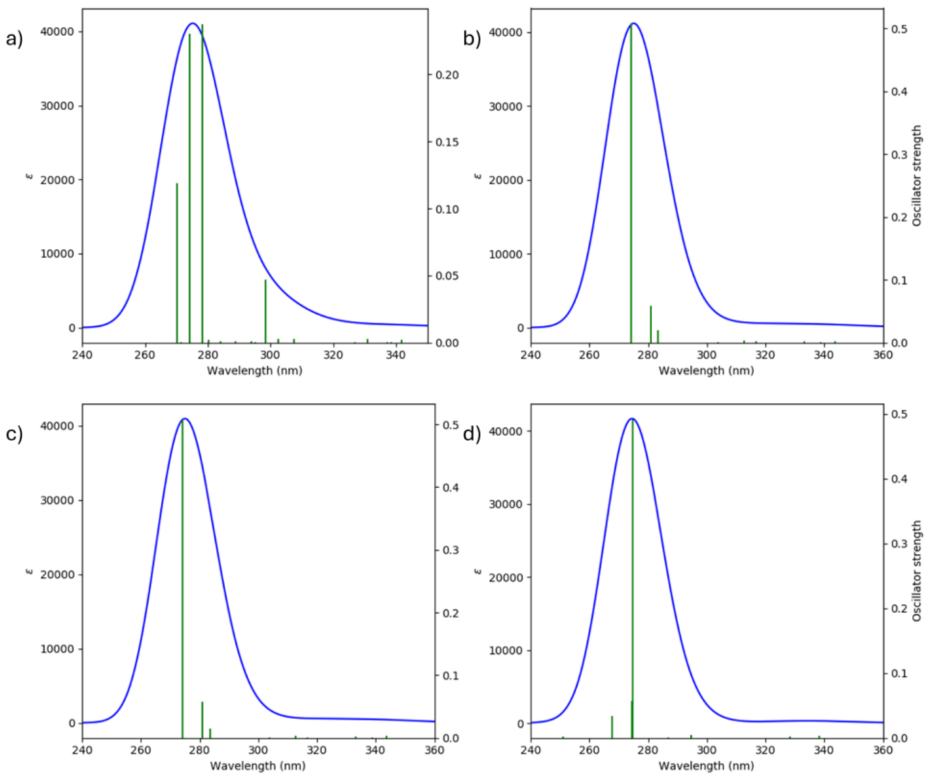

Figure 6. UV-visible absorption of a) Ru-486, b) Ru-486-CH_2CH_3, c) Ru-486-CH_3, d) Ru-486-F molecules

3.5. *UV–Visible analysis*

Using UV spectroscopy and UV-visible spectroscopy, the atomic structure and later the molecular structure were likely first discovered by chemists (Carpentieri & Domenici, 2024). However, optical-based methods have made it easier to examine the optical and electronic properties of nanoscale particles. The principle of UV-Visible analysis relies on the absorption of photons by molecules. When photons with energies in the UV or visible spectrum interact with the sample, electrons in the molecules can transition from lower to higher energy levels (Kebiroglu & Yılmaz, 2023). Figure 6 presents the UV-visible absorption spectra of the Ru-486 molecule and its derivatives, while Table 6 details the absorbance spectra and corresponding peak values for these molecules.

Table 6. Absorbance Spectra and Peaks for RU-486 and Its Derivatives

Figure	Compound	Peak Wavelength (nm)	Energy (eV)	Description
6a	Ru-486	276	4.061	The peak indicates the color of the undoped Ru-486 molecule.
6b	Ru-486-CH_2CH_3	275	4.045	The peak indicates the color of the CH_2CH_3-doped Ru-486 molecule.
6c	Ru-486-CH_3	275	4.044	The peak indicates the color of the CH_3-doped Ru-486 molecule.
6d	Ru-486-F	274	4.081	The peak indicates the color of the F-doped Ru-486 molecule.

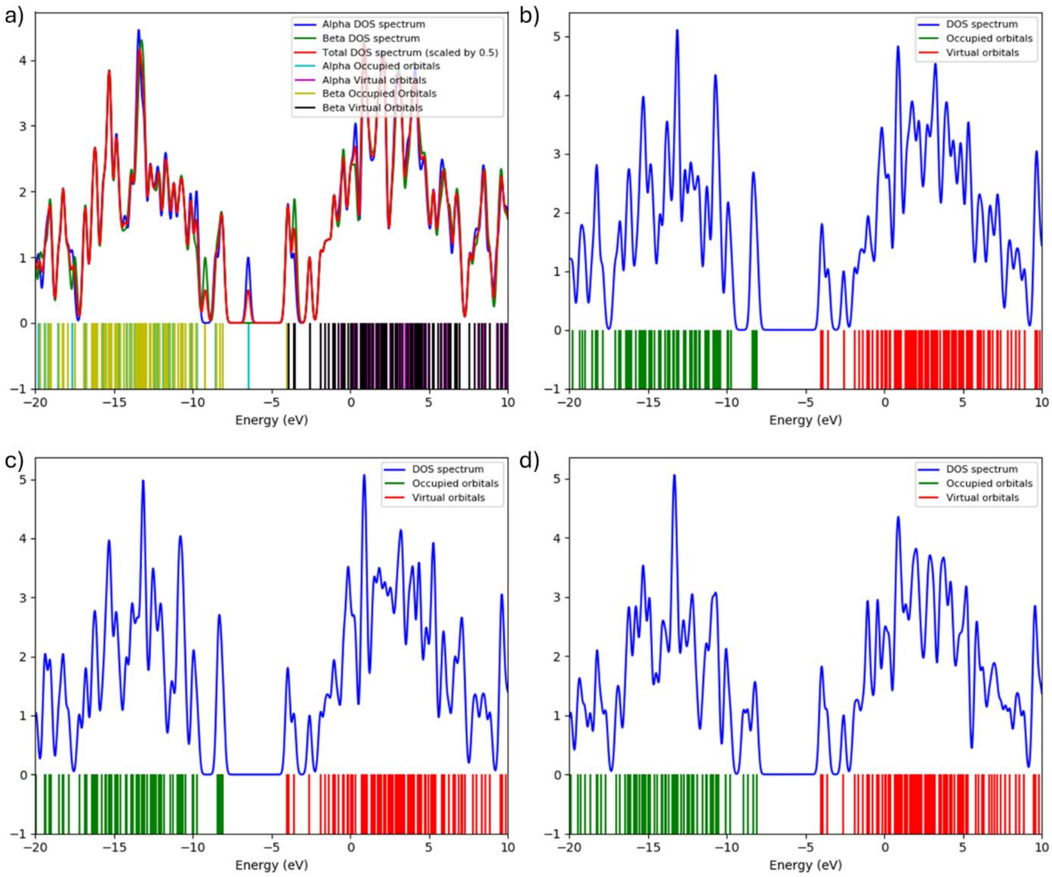

Figure 7. Density of States (DOS) of a) Ru-486, b) Ru-486-CH_2CH_3, c) Ru-486-CH_3, d) Ru-486-F molecules

3.6. *Density of States (DOS)*

The density of states (DOS) is a physical quantity that indicates the number of electronic states at specific energy levels within a material (Erdinc et al., 2024). DOS is a critical parameter in fields such as solid-state physics and materials science for understanding the electronic properties of materials (Hallock & Rose, 2024). Energy (eV) Axis (X-axis): This axis represents the energy levels in electron volts (eV). It ranges from approximately -20 eV to +10 eV. The energy levels are important for understanding the distribution of electronic states within the molecule. DOS Axis (Y-axis): This axis represents the density of states, which indicates the number of electronic states available at each energy level. Color-Coded Spectra: Alpha DOS spectrum (blue): Represents the density of states for alpha spin electrons. Beta DOS spectrum (green): Represents the density of states for beta spin electrons. Total DOS spectrum (red): The combined density of states for both alpha and beta spin electrons, scaled by 0.5 for better visualization. Occupied and Virtual Orbitals: Alpha Occupied orbitals (cyan): Indicates the energy levels where alpha spin electrons are likely to be found in occupied states. Alpha Virtual orbitals (magenta): Indicates the energy levels where alpha spin electrons are likely to be found in virtual (unoccupied) states. Beta Occupied Orbitals (yellow): Indicates the energy levels where beta spin electrons are likely to be found in occupied states. Beta Virtual Orbitals (black): Indicates the energy levels where beta spin electrons are likely to be found in virtual (unoccupied) states. In Figure 7.

4. Conclusions

RU-486 (Mifepristone), combined with misoprostol, is a highly effective and non-invasive method for managing EPL, offering a viable alternative to surgical procedures.

The success of this medical management approach lies in its ability to induce complete uterine evacuation with high efficacy while allowing women to undergo the process in a more private and comfortable setting. The mechanism of action of Ru-486, through progesterone receptor antagonism, cervical ripening, and enhancement of uterine contractions, ensures a comprehensive approach to terminating early pregnancies. The geometry optimization process applied to the Ru-486 molecule and its various derivatives (CH2CH3, CH3, F) provided valuable information about the structural and electronic properties of these compounds. Using the B3LYP-DFT technique with the 6-31G(d) basis set in the Gaussian 09 software package, the most stable, lowest energy conformations were determined for each molecule. Geometry optimization by quantum chemical methods provided a detailed and accurate understanding of the structural and electronic properties of the RU-486 molecule and its derivatives. This understanding is crucial to advance their applications in chemical, pharmaceutical and biological fields and to ensure that these compounds can be effectively used in various practical scenarios. Analysis of Molecular Electrostatic Potential (MEP) maps for Ru-486 molecule and its various derivatives (CH2CH3, CH3, F) summarized the electronic distribution and potential reactive sites in these compounds. The study of MEP maps for Ru-486 and its derivatives highlighted the importance of electrostatic potential analysis in understanding molecular reactivity and interactions. By identifying electrophilic and nucleophilic sites, we can better predict how these molecules will behave in various environments, paving the way for the development of new and more effective chemical and pharmaceutical applications. Vibrational analysis of Ru-486 and its derivatives (CH2CH3, CH3, F) using the DFT/B3LYP method and 6-31G basis set provided important information about the molecular properties and interactions of these compounds. Focusing on estimating their IR spectra and analyzing the absorption peaks in the range of 3500-0 cm^{-1}, it revealed the aspects of their vibrational modes and their corresponding frequencies. By examining different regions of the ^{13}C NMR and ^{1}H NMR spectrum, the presence and effect of various functional groups on the overall molecular structure was determined. UV-Visible spectroscopy analysis of Ru-486 molecule and its derivatives (CH2CH3, CH3, F) provided important information about the electronic transitions and optical properties of these compounds. By examining the absorbance spectra and corresponding peaks, the effects of different functional groups on the electronic structure and optical behavior of Ru-486 molecule were determined. The analysis of Density of States (DOS) for Ru-486 and its derivatives (CH2CH3, CH3, F) provides valuable information about the electronic structure and properties of these molecules. By studying the DOS, we observed the distribution of electronic states at various energy levels, which is crucial for predicting the electronic behavior and reactivity of these compounds. The potential implications for EPL pharmacology have been summarized as bullet points.

Declaration of Ethical Standards

The authors declare that they comply with all ethical standards.

Credit Authorship Contribution Statement

Author 1: Research, Analysis, Writing, Figures and Data.
Author 2: Review and Editing.

Declaration of Competing Interest

The authors have no conflicts of interest to declare regarding the content of this article.

Data Availability

All data generated or analyzed during this study are included in this published article.

Acknowledgement

Mehmet Hanifi KEBİROĞLU is a Ph. D. scholar in computational science and engineering subdivision with a grant of 100\2000 from the council of (YÖK-TURKEY) Higher Education (CoHE) of Türkiye. This article was extracted from the doctoral thesis of Mehmet Hanifi KEBİROĞLU.
I would like to thank my doctoral thesis advisor, Prof. Dr. Niyazi BULUT, for his valuable contributions to this article.

5. References

Akter, S., Rahman, J., & Ara, A. M. (2024). Termination of Unwanted Pregnancy by Medication (Mifepristone and Misoprostol). *Sch Int J Obstet Gynec*, 7(4), 148-154. https://doi.org/110.36348/sijog.2024.v07i04.00

Alejandro, A. (2024). The Generation of Terahertz Light and its Applications in the Study of Vibrational Motion. *Theses and Dissertations*. 10330

Bae, S., & Kim, D. (2024). Improving home-like environments in long-term care units: an exploratory mixed-method study. *Scientific Reports*, 14(1), 13243. https://doi.org/10.1038/s41598-024-62328-0

Biswas, S., Sengupta, M., Ghosh, D., & De Rajesh, R. (2024). Induction of abortion in the first trimester of pregnancy using letrozole and misoprostol combination versus misoprostol alone-A comparative observational study. *Asian Journal of Medical Sciences*, 15(1), 94-101. https://doi.org/10.3126/ajms.v15i1.58935

Butera, V. (2024). Density functional theory methods applied to homogeneous and heterogeneous catalysis: a short review and a practical user guide. *Physical Chemistry Chemical Physics*. https://doi.org/10.1039/D4CP00266K

Carpentieri, M. A., & Domenici, V. (2024). Introducing UV–visible spectroscopy at high school level following the historical evolution of spectroscopic instruments: a proposal for chemistry teachers. *Foundations of Chemistry*, 26(1), 115-139. https://doi.org/10.1007/s10698-024-09501-5

Chakrawal, A., Lindahl, B. D., Qafoku, O., & Manzoni, S. (2024). Comparing plant litter molecular diversity assessed from proximate analysis and 13C NMR spectroscopy. *Soil Biology and Biochemistry*, 109517. https://doi.org/10.1016/j.soilbio.2024.109517

Chua, H. S., Saw, Z. K., & Mohd-Said, S. (2024). Implementing the 2017 EFP/AAP Periodontal Disease Classification in The Diagnosis and Management of Endo-Periodontal Lesions: A Case Report. *Cakradonya Dental Journal*, 16(1), 17-23. https://doi.org/10.24815/cdj.v16i1.36416

Çankaya, N., Kebiroğlu, M. H., & Temüz, M. M. (2024). A comprehensive study of experimental and theoretical characterization and in silico toxicity analysis of new molecules. *Drug and Chemical Toxicology*, 1–15. https://doi.org/10.1080/01480545.2024.2353724

Elia, A., Pataccini, G., Saldain, L., Ambrosio, L., Lanari, C., & Rojas, P. (2024). Antiprogestins for breast cancer treatment: We are almost ready. *The Journal of Steroid Biochemistry and Molecular Biology*, 241, 106515. https://doi.org/10.1016/j.jsbmb.2024.106515

Engstrom, T., Shteiman, M., Kelly, K., Sullivan, C., & Pole, J. D. (2024). What is measured matters: A scoping review of analysis methods used for qualitative patient reported experience measure data. *International Journal of Medical Informatics*, 105559. https://doi.org/10.1016/j.ijmedinf.2024.105559

Erdinc, F., Gulebaglan, S. E., & Doğan, E. K. (2024). Revealing Structural, Electronic and Elastic Properties of NaPaO3 compound theoretically. *International Journal of Medicine and Occupational Health and Safety Sciences*, 2(1). https://doi.org/10.5281/zenodo.12598795

Genoni, A., & Martín Pendás, Á. (2024). Critical assessment of the x-ray restrained wave function approach: Advantages, drawbacks, and perspectives for density functional theory and periodic ab initio calculations. *The Journal of Chemical Physics*, 160(23). https://doi.org/10.1063/5.0213247

George-Carey, R., Memtsa, M., Kent-Nye, F. E., Magee, L. A., Oza, M., Burgess, K., ... & Silverio, S. A. (2024). Women’s experiences of early pregnancy loss services during the pandemic: a qualitative investigation. Women and Birth, 37(2), 394-402. https://doi.org/10.1016/j.wombi.2023.12.004

Gidado, A. S., Ahmad, S. K., Musa, A., & Ibrahim, U. M. (2024). Determination of the Electronic Structure, Charge-transfer, and Optical Properties of Neutral, Anionic, and Cationic Perfluoropentacene. *Chemical Science International Journal*, 33(4), 54-68.

Hallock, C. D., & Rose, M. J. (2024). Electrochemical Impedance of Well-Passivated Semiconductors Reveals Bandgaps, Fermi Levels, and Interfacial Density of States. *Journal of the American Chemical Society, 146* (28), 18989-18998 https://doi.org/10.1021/jacs.4c02738

Hogmark, S. (2024). Meeting the needs of women: provision of long-acting reversible contraception at the time of abortion. Inst för kliniska vetenskaper, *Danderyds sjukhus/Dept of Clinical Sciences, Danderyd Hospital*. https://hdl.handle.net/10616/49006

Holehouse, A. S., & Kragelund, B. B. (2024). The molecular basis for cellular function of intrinsically disordered protein regions. *Nature Reviews Molecular Cell Biology*, 25(3), 187-211. https://doi.org/10.1038/s41580-023-00673-0

Kay, J. E., Brody, J. G., Schwarzman, M., & Rudel, R. A. (2024). Application of the key characteristics framework to identify potential breast carcinogens using publicly available in vivo, in vitro, and in silico data. *Environmental Health Perspectives*, 132(1), 017002. https://doi.org/10.1289/EHP13233

Kebiroglu, H., & Ak, F. (2023). Molecular Structure, Geometry Properties, HOMO-LUMO, and MEP Analysis of Acrylic Acid Based on DFT Calculations. *Journal of Physical Chemistry and Functional Materials*, 6(2), 92-100. https://doi.org/10.54565/jphcfum.1343235

Kebiroglu, H., & Yılmaz, M. (2023). Investigation of UV-Visible Absorption Quantum Effects Doped of Norepinephrine, Mg+2 Atom by Using DFT Method. *Journal of Physical Chemistry and Functional Materials*, 6(2), 145-151. https://doi.org/10.54565/jphcfum.1332113

Kolek, P., Andrzejak, M., Uchacz, T., Goclon, J., Pogocki, D., Kisała, J., ... & Tulej, M. (2024). LIF spectrum for the localised S0→ S1 (ππ*) excitation in the H-bonded anthranilic acid dimer: Symmetry breaking or coupling of vibrations. *Spectrochimica Acta Part A: Molecular and Biomolecular Spectroscopy*, 319, 124491. https://doi.org/10.1016/j.saa.2024.124491

La Marca, A., & Diamanti, M. (2024). Factors affecting age at menopause and their relationship with ovarian reserve: a comprehensive review. *The European Journal of Contraception & Reproductive Health Care*, 1-11. https://doi.org/10.1080/13625187.2024.2375281

Lewars, E. G. (2024). Ab initio calculations. In Computational Chemistry: Introduction to the Theory and Applications of Molecular and Quantum Mechanics (pp. 199-432). *Cham: Springer International Publishing*. https://doi.org/10.1007/978-3-031-51443-2_5

Margraf, J. T. (2024). Neural graph distance embedding for molecular geometry generation. *Journal of Computational Chemistry,* 45(21), 1784. https://doi.org/10.1002/jcc.27349

Marwah, S., Gupta, S., Batra, N. P., Bhasin, V., Sarna, V., & Kaur, N. (2016). A comparative study to evaluate the efficacy of vaginal vs oral prostaglandin E1 analogue (Misoprostol) in management of first trimester missed abortion. *Journal of clinical and diagnostic research: JCDR*, 10(5), QC14. https://doi.org/10.7860/JCDR/2016/.7891

McCullya, B., Dodampahalaa, S. H., Menonb, A. S., D'Sab, N., Dayb, E., Ahmedb, M., & Rahimb, M. M. (2024). Management and clinical implications of multiple pregnancies: A focus on zygosity, chorionicity, and monochorionic twin complications, Sri Lanka Journal of Obstetrics and Gynaecology, 46, 1, 21-31 https://doi.org/10.4038/sljog.v46i1.8131

Nguyen, T. (2024). Impacts of basis sets, solvent models, and NMR methods on the accuracy of 1H and 13C chemical shift calculations for biaryls: a DFT study. *Science and Technology Development Journal*, 27(1), 3339-3346. https://doi.org/10.32508/stdj.v27i1.4182

Pedraza, E. C., Vokinger, A. K., Cleves, D., Michel, G., Wrigley, J., Baker, J. N., ... & McNeil, M. J. (2024). Grief and bereavement support for parents in low- or middle-income countries: a systematic review. *Journal of Pain and Symptom Management*, 65, 5, e453-e471. https://doi.org/10.1016/j.jpainsymman.2024.01.023

Pellegrini, C., & Sanna, A. (2024). Ab initio methods for superconductivity. *Nature Reviews Physics*, 1-15. https://doi.org/10.1038/s42254-024-00738-9

Qin, Y., Touch, K., Sha, M., Sun, Y., Zhang, S., Wu, J., ... & Xiao, J. (2024). The chromosomal characteristics of spontaneous abortion and its potential associated copy number variants and genes. *Journal of Assisted Reproduction and Genetics*, 1-12. https://doi.org/10.1007/s10815-024-03119-4

Rahman, M. U., Khan, S., Khan, H., Ali, A., & Sarwar, F. (2024). Computational chemistry unveiled: a critical analysis of theoretical coordination chemistry and nanostructured materials. *Chemical Product and Process Modeling*. 19, 4, 473-515. https://doi.org/10.1515/cppm-2024-0001

Reeda, V. J., Sakthivel, S., Divya, P., Javed, S., & Jothy, V. B. (2024). Conformational stability, quantum computational (DFT), vibrational, electronic and non-covalent interactions (QTAIM, RDG and IGM) of antibacterial compound N-(1-naphthyl) ethylenediamine dihydrochloride. *Journal of Molecular Structure*, 1298, 137043. https://doi.org/10.1016/j.molstruc.2023.137043

Riddell, G. (2024). Early Pregnancy Loss. *Collins-Bride & Saxe's Clinical Guidelines for Advanced Practice Nursing*, 231.

Statham, H. (2002). Prenatal diagnosis of fetal abnormality: the decision to terminate the pregnancy and the psychological consequences. *Fetal and Maternal Medicine Review*, 13(4), 213-247. https://doi.org/10.1017/S0965539502000414

Suhta, A., Saral, S., Çoruh, U., Karakuş, S. E. V. G. İ., & Vazquez-Lopez, E. M. (2024). Synthesis, Single Crystal X-Ray, Hirshfeld Surface Analysis and DFT Calculation Based NBO, HOMO–LUMO, MEP, ECT and Molecular Docking Analysis of N′-[(2, 6-Dichlorophenyl) Methylidene]-2-{[3-(Trifluoromethyl) Phenyl] Amino} Benzohydrazide. *Journal of Structural Chemistry*, 65(1), 196-215. https://doi.org/10.1134/S0022476624010189

Tagliavini, E., Decesari, S., Paglione, M., & Mazzanti, A. (2024). NMR spectroscopic applications to atmospheric organic aerosol analysis–Part 2: A review of existing methodologies and perspectives. *TrAC Trends in Analytical Chemistry*, 117595. https://doi.org/10.1016/j.trac.2024.117595

Tegegn, D. F., Belachew, H. Z., & Salau, A. O. (2024). DFT/TDDFT calculations of geometry optimization, electronic structure and spectral properties of clevudine and telbivudine for treatment of chronic hepatitis B. *Scientific Reports*, 14(1), 8146. https://doi.org/10.1038/s41598-024-58599-2

Tisato, V., Silva, J. A., Scarpellini, F., Capucci, R., Marci, R., Gallo, I., ... & Gemmati, D. (2024). Epigenetic role of LINE-1 methylation and key genes in pregnancy maintenance. *Scientific Reports*, 14(1), 3275. https://doi.org/10.1038/s41598-024-53737-2

Turner, J. V., Garratt, D., Barwick, A., McLindon, L. A., Spark, M. J., & Smith, A. (2024). Congenital and Fetal Effects After Mifepristone Exposure and Continuation of Pregnancy: A Systematic Review. *Clinical Pharmacology & Therapeutics*. 116: 1207-1216. https://doi.org/10.1002/cpt.3392

Viganò, S., Smedile, A., Cazzella, C., Marra, P., Bonaffini, P. A., & Sironi, S. (2024). Abnormal Uterine Bleeding: A

Pictorial Review on Differential Diagnosis and Not-So-Common Cases of Interventional Radiology Management. *Diagnostics*, 14(8), 798. https://doi.org/10.3390/diagnostics14080798

Yang, X., Wang, R., Zhang, W., Yang, Y., & Wang, F. (2024). Predicting risk of the subsequent early pregnancy loss in women with recurrent pregnancy loss based on preconception data. *BMC Women's Health*, 24(1), 381. https://doi.org/10.1186/s12905-024-03206-9

Ye, A., Li, L., Chen, H., Tao, P., & Lou, S. (2024). Nicotine regulates abnormal macrophage polarization and trophoblast invasion associated with preterm labor via the α7nAChR/SIRT1 axis. *Placenta*, 147, 42-51. https://doi.org/10.1016/j.placenta.2024.01.014

Yılmaz, M., & Kebiroglu, H. (2024). Nuclear Magnetic Resonance and Quantum Chemical Calculations of Ca+2 Doped Norepinephrine Molecule by Using DFT and HF Methods. *International Journal of Pure and Applied Sciences*, 10(1), 1-11. https://doi.org/10.29132/ijpas.1376725